

USRP based X-band Digital Beam Forming Synthetic Aperture Imaging Radar

P. Stenger
Electrical Design Technology
Northrop Grumman Corp.
Baltimore, MD, USA
peter.stenger@ngc.com

M. Blue
Mechanical Technology
Northrop Grumman Corp.
Baltimore, MD, USA
Michael.blue@ngc.com

M.Urdareanu
FAMU-FSU College of
Engineering
Tallahassee, FL. USA
mgu15@my.fsu.edu

G. Steans
FAMU-FSU College of
Engineering
Tallahassee, FL. USA
grant1.steans@famu.edu

N. Henry
FAMU-FSU College of
Engineering
Tallahassee, FL. USA
njh16d@my.fsu.edu

T. Lewis
FAMU-FSU College of
Engineering
Tallahassee, FL. USA
tl14@my.fsu.edu

Abstract— A Universal Software Radio Peripheral (USRP) transceiver is investigated as a digital radar transceiver in an elemental digital beam forming (DBF) up/down converter scheme at X-band that images a scene spatially with signal time division multiplexing (TDM) implemented across multiple input-output (MIMO) transmit-receive elements. This forms a synthetic aperture radar (SAR) image of the scene with no moving parts. A wide instantaneous bandwidth (IBW) of 44.8 MHz is achieved with an Ettus Research B200 USRP that transmits and receives linear frequency modulated (LFM) pulses that are synchronized between two transmit antenna elements and eight receive antenna elements forming 16 virtual elements that resolve 1.17 degrees of spatial angular resolution across +/- 8.75 degrees of unambiguous field of view. A peripheral commercial Field Programmable Gate Array (FPGA) evaluation board is used to generate a one pulse per second (1PPS) timing signal to synchronize the USRP generated waveform with the RF switches that excite each transmit/receive virtual element. A commercial component based up/down converter front end extends the RF carrier frequency of the USRP to 10 GHz at each switched aperture element.

Keywords—FMCW radar, MIMO virtual array, USRP, GNU

I. INTRODUCTION

Low cost USRP [4] radio technology offers a cost effective solution for radar back end implementations supporting fundamental RF frequencies up to 6 GHz and higher as an IF frequency that can be used to up-convert to much higher operating frequencies. These units can generate baseband arbitrary waveforms onto an RF carrier in the digital domain at modest bandwidths (50 MHz) and also receive the full bandwidth for digital demodulation. Prior work in [1] implemented a 28 MHz IBW FMCW waveform with a B210 for range-Doppler mapping from a single bi-static aperture at a carrier frequency of 2.2 GHz. A single axis SAR radar was

demonstrated in [2] by students at MIT using TDM between MIMO transmit and receive elements at 2.4 GHz with an FMCW waveform generated from a voltage controlled oscillator covering 80 MHz of bandwidth. This paper implements an up/down conversion scheme for operation at much higher carrier frequency of 10 GHz, in a two axis TDM-MIMO scheme that uses SAR image formation.

Ease of programming with GNU Radio Companion (GRC) [4] allows programming of the USRP modulation and demodulation functions in a simple user-friendly graphical user interface (GUI) application with an extensive pallet of different signal processing functions [3]. Primary sources of information for basic GNU Radio can be found at <https://www.gnuradio.org/> and <https://wiki.gnuradio.org/index.php/GNURadioCompanion>. The USRP units are very affordable (<\$1000) making them a valuable learning tool for signal systems education and are ideal for academic undergraduate senior design projects in universities that offer electrical and computer engineering programs. This work, sponsored by Northrop Grumman Corp., was done by seniors as part of their undergraduate senior design class project in electrical and computer engineering at Florida Agricultural & Mechanical University and Florida State University (FAMU-FSU) College of Engineering, both in Tallahassee, FL. All the required USRP software is free open source software (FOSS) readily downloaded from the internet. In the past expensive test equipment was used to generate and receive signals to demonstrate this type of radar. USRPs operating with GNU Radio FOSS can support multiple signal analysis functions such as an oscilloscope and spectrum analyzer for signal verification. A vector Fourier Transform (FFT) is also supported that can measure the phase locked amplitude and phase of a signal [4].

A. System and Aperture Design

System concept of operation, illustrated in Fig 1, provides three dimensions of spatial resolution. Two dimensions in

cross range and one dimension down-range of a scene using a pulsed X-band signal modulated with an LFM [1] [5] waveform within each pulse covering 44.8 MHz of IBW over an individual pulse width of 10.24 us.

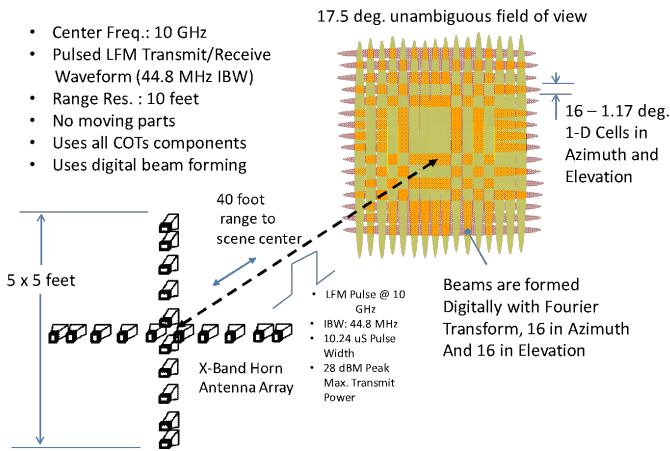
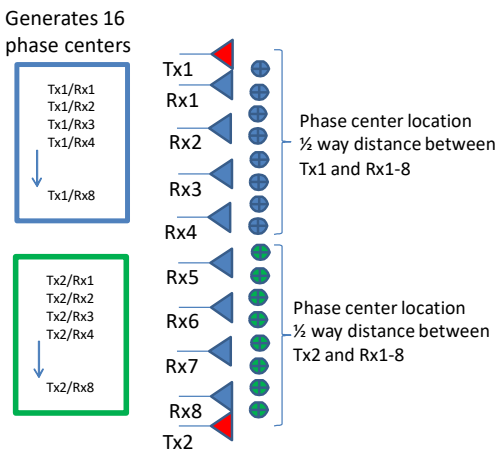


Fig. 1. Imaging Radar 2-D Operational Concept. Union of the orthogonal 1-D images forms 2-D image of scene

The pulses are long, spanning over 10,000 feet during one-way propagation compared to the 40 foot scene range being measured. Therefore transmission and reception in the USRP occurs at the same time over most of the frequency modulated pulse duration at these short ranges as in FMCW radars [5]. Eight receive horns in each axis are used to form 16 virtual phase centers enabling beam forming of the scene with no moving parts. A single receive horn is used during each TDM data collection transmission. Fig. 2 shows the aperture design and how 16 virtual phase centers are formed in an axis by activating specific transmit/receive pairs [2].



Two transmit horns, on the ends of an eight element line array each switch through eight receive horns forming 16 virtual phase centers [2]. To minimize the cost of the Commercial off the Shelf (COTS) antennas, the aperture radiators were procured commercially and manufactured in plastic with metal tin plating at cost of \$20 each [2]. Fig. 3 shows a photo of the aperture assembly that is built from lightweight T-slotted, aluminum extrusions provided by 80/20 Inc. The line arrays are formed by radiators that are mounted at specific positions along the slotted frame members. Additionally, the system is easily transported and configured using integral locking

Fig. 2. Sixteen Synthetic Aperture 1-D Phase Centers at 3λ spacing formed for each axis

wheels and standard interfaces. Components are mounted with screws to base of electronics module and interconnected with shielded coax. The width of the flared openings of the waveguide horns dictated the minimum spacing that could be achieved between the antennas to form the widest unambiguous field of view. This resulted in a 3λ spacing at 10 GHz between the end transmit and neighboring receive horns, and 6λ between the remaining receive horns. This configuration as shown in Fig. 2 creates 16 virtual phase centers at a 3λ spacing in one axis (azimuth) that enables an unambiguous +/-8.75 degree field of view with a spatial resolution and formation of 16 digitally formed beams at a sector increment of 1.17 degrees in one dimension. Each horn

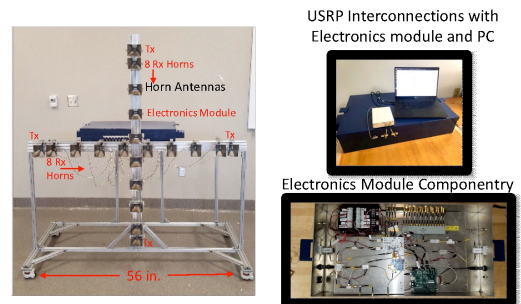


Fig. 3. Integrated Electronics Hardware Photos

has a beam-width of 25 degrees completely covering the +/- 8.75 degree field of view. The same configuration is used in the orthogonal axis (elevation) creating a similar 1-dimension image. Forming the intersecting union of the 2 images can provide a 2-dimension spatial image of where the scattering energy is located in azimuth and elevation. This simple approach can result in ambiguities if there are scatterers of the same magnitude in the same range cell. Image formation with a two dimensional complex Fourier transform of the aperture distribution can also be used which eliminates the ambiguity however results in higher image side-lobes. Additional MIMO states between the vertical and horizontal arrays can increase the fill factor and reduce side-lobes.

System components [4] are shown in Fig. 4 where during transmission the final radiated X-band signal is up converted from a 2.2 GHz carrier signal generated by the USRP. A separate oscillator signal at 7.8 GHz is divided between the up conversion mixer and the down conversion mixer for a phase coherent system. The received signal following down conversion to the 2.2 GHz IF carrier is received, digitized and recorded by the USRP. The FPGA controls the switching timing between transmit and receive pairs and is synchronized with the pulses from the USRP. The team designed a chain of COTs RF components, which would give the expected power for transmit and expected gain for receive.

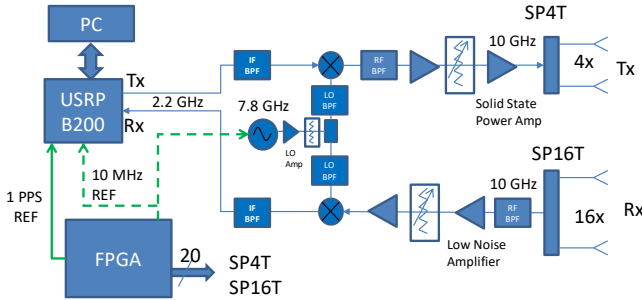


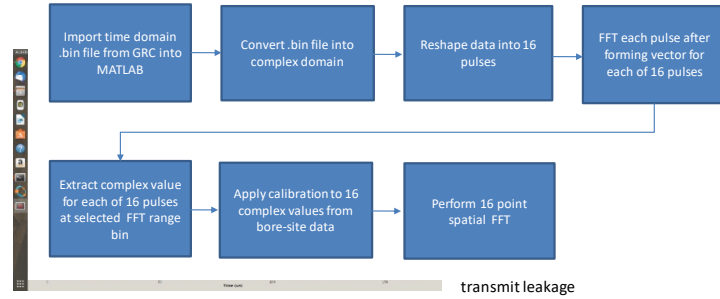
Fig. 4. All Commercial Components Used In Electrical Design

The initial frequency plan was implemented using a signal generator for the local oscillator signal to verify the up and down conversion performance. Measurements were made to ensure each RF component in the chain was outputting the desired power or gain before the next part of the chain was added. Once it was determined that the chain was giving the expected power, the local oscillator signal generator was replaced with a commercially available Texas Instruments RF Synthesized Source evaluation board. The source was programmed using TICS Pro, a software application for setting the appropriate center frequency of 7.8 GHz. To produce the desired power required for the chain, the system was setup so the USRP B200 radio generated a 2.2 GHz center frequency at 3 dBm peak and the synthesizer board generated 7.8 GHz at 7 dBm for the local oscillator drive.

II. USRP RADAR WAVEFORM GENERATION AND RECEPTION

The radar waveform generated and received by the USRP is a train of linear frequency modulated (LFM) pulses, each with a bandwidth of 44.8 MHz generated at a sample rate of 50MHz [1][3]. The complex binary file waveform is generated using MATLAB and is then repeated sixteen times, for a total of 16 pulses necessary for the 16 transmit-receive horn pairs. This is stored in a binary file such that the USRP can read it in. A delay of 8 samples (160 ns) is added between each pulse, to allow for switching the aperture from one transmit-receive

pair to another. Fig. 5 shows the GNU Radio display providing visualization of the pulse waveforms as a function of time at key points in the RF thread.



Two Corner Reflectors (CRs) + Transmit leakage

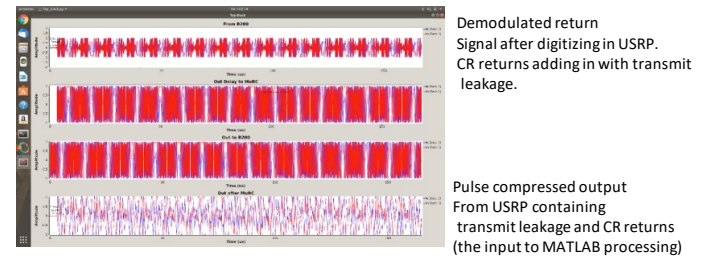


Fig. 5. Displayed data from the USRP in the GRC shows sixteen LFM pulses at key points in the signal thread

The transmission and reception of the signals is controlled by the GRC flow graph shown in Fig, 6 running at a sample rate of 50 MHz.[1]. The scattered return signal from the scene is digitized in the USRP and a digital de-ramp pulse compression function [5] is performed that resolves range by multiplying it with a conjugated version of the original signal to achieve pulse compression. The signal is then saved to a binary file for analysis in MATLAB. Each data collection dwell contains 16 pulses that are stored in the sink file block prior to MATLAB processing. Attempts were made to do continuous streaming through the USRP, however the USB3.0 port was not fast enough at the 50 MHz sample rate to avoid

sample dropouts, therefore single 16 pulse data set collects were used that were sufficient for radar operations.

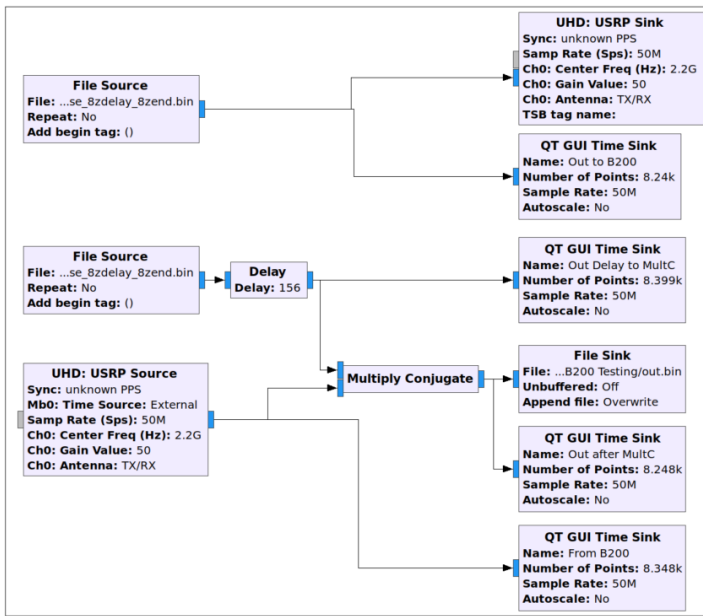


Figure 6. GNU radio flow graph programs USRP transceiver function including the conjugate multiply that performs digital pulse compression at the full IBW (44.8 MHz) for each of the 16 pulses in a data collection set

III. MATLAB DIGITAL SIGNAL PROCESSING

The output values from GRC were imported into MATLAB as an array of 8,192 complex values that contained all 16 pulses for one complete axis data collection. Fig. 7 shows the signal processing flow for image formation. A major portion of our project was analyzing various data points to ensure the accuracy of our results. Without this verification step, the team would never be able to fine tune transmit and receive aperture alignment for proper functionality. Understanding how the aperture collects data is key to understanding the difference between the good results and bad results. We observed through various test that we were able to more accurately represent the spatial position of our metal reflectors when the generated phase plots, from a corner reflector directly centered in our field range at boresight, had a relatively symmetric form. This resulted in subsequent data collects producing more accurate results. The phase symmetry insures that the synchronization of the signal reflection received was even across all 16 receive horns. This results in a steady and even switching sequence.

The next step taken in process was ensuring consistent signal strength from the receive horns. This was accomplished by

shaping the complex value array into sixteen individual arrays to represent our sixteen pulses. The time domain data is processed through the MATLAB FFT function to analyze the coefficient magnitudes of each individual pulse at specific frequency bins that correspond to range. With this representation we are able to distinguish two peaks at separate range bins; one from signal leakage directly from the transmit horns and another from the signal reflected back by our metal corner reflectors. Verifying that the peaks observed occur at the same bin location consistently across all sixteen pulses is

Fig. 7. Processing flow in MATLAB after digitally pulse compressed complex baseband data is obtained from the USRP

critical to verifying bin energy is from same range. Fig. 8 shows a typical FFT of one of the pulses that contains the transmit leakage and the desired return signal bin. The FFT isolates the leakage and allows the desired signal complex characteristics to be obtained. This validates that the incoming signal is being detected at the same relative distance through each receive horn, and that the aperture is operating properly.

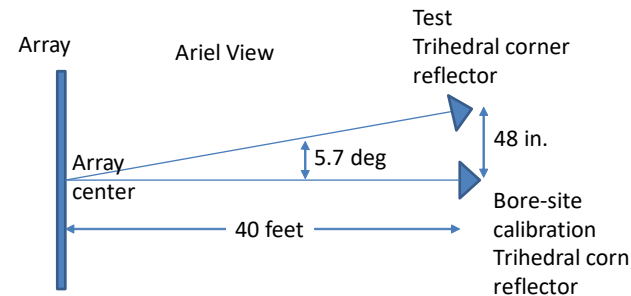
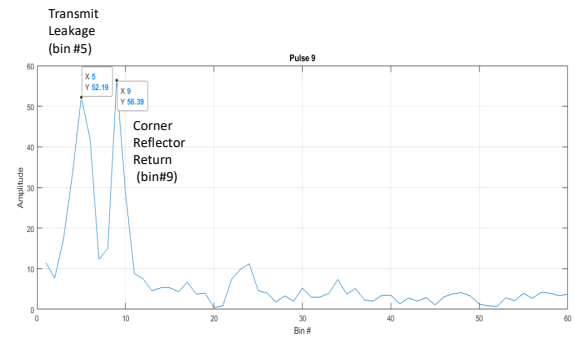


Fig. 9. Simple scene with corner reflectors used to verify Fundamental system performance with minimal scattering variables in scene. All other scatterers are many range cells away so reflectors can be identified in range cells

After giving validation to the data received, the sixteen pulse matrix is processed using a MATLAB script developed by the team that calculates the real and imaginary part for each of the sixteen bins. The last step prior to the final spatial Fourier transform that produces the image involves calibrating the measured data with the boresight measurement. This removes the hardware RF insertion phase, amplitude errors in

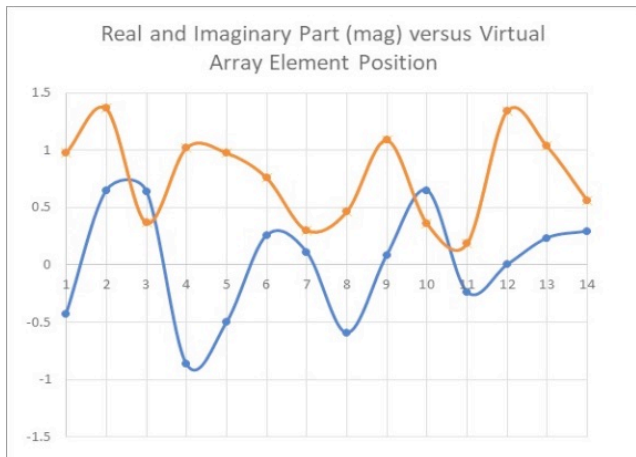
the different paths and the different path lengths between receive horns and the scene. The calibration performs a complex conjugate multiply to normalize the phase, and a divide by amplitude normalization for amplitude with the boresight data. An important verification during this process was that the phase of the signal across all the pulses was stable within few degrees for a test case where we used an 8-way RF divider to feed eight switch input ports with a common transmit signal phase. The other factor worth noting is that during each data collect the phase of the radio starts at a different phase when generating the sixteen pulses. When the calibration is applied that zeroes the imaginary part of the calibration data, it is applied during the scene data collection where the radio produces a different starting phase. The relative phase stays the same though and the calibration results in a constant phase other than zero across all the virtual elements with no phase slope therefore the calibration factors still result in an accurate measurement.

IV. APERTURE TIMING AND CONTROL

Accurately controlling the timing of the switches that activate the transmit-receive paths with the arrival of the pulse waveform was a key challenge. This was satisfied by using an FPGA [4] to generate a 1PPS timing signal that was used as the reference for the FPGA and the USRP which is designed to receive a 1PPS signal normally from a GPS receiver. There was an extra delay that had to be added to account for producing the USRP signal at the connector relative to the signal activation from GRC. A better future implementation would be to RF detect the USRP signal and use that detected edge as a reference to start the FPGA switch timing. A commercial FPGA demonstration board, the NEXYS3 Diligent was used.

V. MEASUREMENT RESULTS AND CALIBRATION

Measurement data was collected from trihedral corner reflectors (CRs) located in the field of view at a range of about 40 ft. The scene layout is shown in Fig. 9. Note that at a 40 foot range the CR is not in the far field, therefore the path length will be different to each virtual element since the virtual array is electrically long at 10 GHz (45λ) compared to

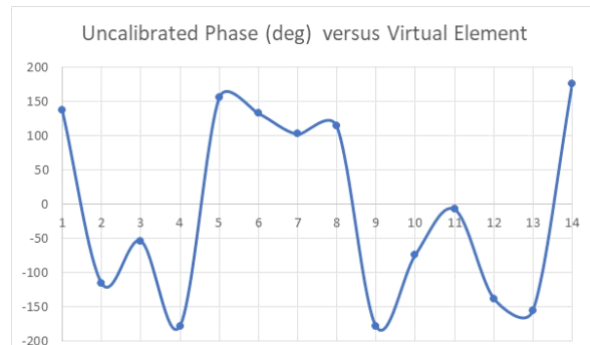


the 40 ft range which is 407λ . This needs to be accounted for

Figure 10. Measured phase versus virtual element of single reflector at bore site. Note symmetry of phase around boresite as expected since virtual elements are symmetric around boresite. This data is used as boresite calibration data.

as a phase calibration factor at this short range.

The first test involved calibrating these path length differences and the different RF hardware paths through the RF switches compensating for the different amplitude and phases since all 16 paths are physically different, even though they are designed and implemented to be matched with identical cable lengths. To this end a single CR was mechanically aligned at boresight and then measured with the radar to obtain these calibration values which were then applied to all future data. The measured pre-calibration raw phase versus element position of the 10 GHz signal, as shown in Fig. 10, was surprisingly symmetric indicating there were well balanced RF paths through each switch path and the array was aligned well to the corner reflector. This data was extracted from the FMCW compressed range bin in the Fourier transform corresponding the 40 foot range response. The transmit to receive FMCW leakage signal feeds directly across transmit and receive horns at aperture, and is easily removed from the measurement given the wide 44.8 MHz bandwidth that enables range resolutions of 10 feet.



However the receive horn next to each transmit horn was overcome by too much leakage signal, due to its close proximity, and was not able to produce a detection at the 40 ft range. We attributed this to saturation of the receive path that might be occurring when the receive antenna activated is next to transmit. Therefore the outer most spatial virtual elements were omitted from the measured data set and the complex-valued discrete Fourier transform (DFT) was reduced to 14 points in the 16 point DFT calculation (first point and last

point were zero valued), for digital beam forming and image formation. A simple calibration of the single CR boresight data involving a complex conjugate multiply to normalize the phase, and a divide by amplitude normalization for amplitude was applied to subsequent data. Note that at a range of 40 feet the path length error will not be the same at other angles off boresight. Since the field of view was fairly narrow (± 8.75 degrees), it was calculated that a CR kept on a radius of 40 ft when testing a CR off boresight, resulted in minimal error when the boresight path length calibration error was applied. This also allows the result produced by the Fourier transform, which assumes far field ranges, to be used for the digital beam forming with small error.

Fig. 11. Measured real and imaginary part with both reflectors and the bore-site calibration applied.

The goal of the next test was to bring a second corner reflector into the left side (negative angle side) of the scene which was located off boresight at a -5.7 degree angle on the 40 foot radius, and show measured data would include the 2nd CR such that both the CR at boresight and the 2nd CR would be visible in the digitally-formed scene when processed through spatial DFT. The boresight calibration factors were applied to the data with both corner reflectors in the scene which resulted amplitude and phase values for each phase center that were then decomposed using the complex spatial DFT to form beams representing angle of arrival. Fig. 11 shows the measured real and imaginary part response versus virtual element after calibration was applied, where the expected sinusoid response is obtained for the real and imaginary parts. The periodicity of this phase was decomposed with complex basis functions in a 16 point DFT into angle space resulting in a response at -5.4 degrees and equal responses at $+0.6$ and -0.6 degrees. Since there are an even number of virtual element phase centers, boresight produces response at both -0.6 degrees and $+0.6$ degrees. Fig. 12 shows the digitally formed image versus angle after Taylor weighting [5] is applied showing a response at -5.4 degrees (the second corner reflector) and responses at -0.6 and $+0.6$ degrees since the calibration CR was at 0 degrees boresight. With an even number of virtual element phase centers, 0 degrees is not occupied so response is shared between the 0.6 and -0.6 angles. Given the limited time associated with the spring college semester, additional measurements beyond the single axis were not able to be made. The fundamental result shown in Fig. 12 with the two CRs show that accurate image formation was demonstrated and that the radar system met primary functional goals.

Amplitude (dB) versus Angle (degrees)

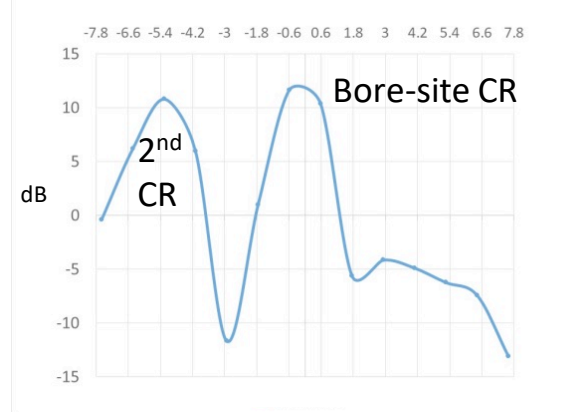


Fig. 12. Measured results of final spatial FFT with Taylor weighting that produces angle of arrival in image plane of for both reflectors in scene. 2nd CR is measure at -5.4 degrees off bore-site. This was very close to the off bore-site mechanical angle of 5.7 degrees. The expected and measured are both within the angular FFT resolution cell centered at 5.25 ± 0.6 degrees

VI. CONCLUSIONS

A commercial USRP transceiver [1] [3] was successfully used as the back-end radar exciter/receiver in a digital beam forming synthetic aperture antenna array that uses TDM and MIMO methods. The USRP provided a sequence of phase coherent 16 RF pulses each modulated with an LFM waveform at a modest sample rate of 50 MHz (44.8 MHz IBW). The USRP digitized the received pulses and performed the pulse compression prior to storing in a binary file for subsequent processing. USRPs are a cost effective way to generate and receive modest bandwidth signals on an RF carrier. All the USRP software is FOSS enabling a very cost effective way to implement experimental radar systems in the future. An alternative that avoids the licensing costs of MATLAB is Linux Octave, a FOSS application.

ACKNOWLEDGMENT

The authors would like to thank the numerous undergraduate students from past senior design classes at FAMU/FSU College of Engineering for their contributions. Special thanks to Dr. Jerris Hooker for his academic support, Prof. Simon Foo for allowing continued research in this area and the overall support from the FAMU-FSU College of Engineering. Finally, the authors would like to acknowledge the Northrop Grumman Corp. in Baltimore Maryland for their continued monetary support for materials that enabled advancing this project to the point of successful demonstration

REFERENCES

- [1] T. W. Mathumo, T. G. Swart, and R. W. Focke, "Implementation of a GNU Radio and Python FMCW radar toolkit," in *IEEE AFRICON*, Cape Town, South Africa, Sept. 18–20, 2017.
- [2] B. T. Perry, T. Levy, P. Bell, S. Davis, K. Kolodziej, N. O'Donoghue, and J. S. Herd, "Low cost phased array radar for applications in engineering education," in *IEEE International Symposium on Phased Array Systems and Technology*, Waltham, MA, Oct. 15–18, 2013, pp. 416–420.
- [3] J. Ralston, and C. Hargrave, "Software defined radar: an open source platform for prototype GPR development," in 14th International Conference on Ground Penetrating Radar (GPR), Shanghai, China, June 4–8, 2012, pp. 172–177.
- [4] D. M. Chinnam, J. Madhusudhan, C. Nandhini, S. N. Prathyusha, S. Sowmiya, R. Ramanathan, and K. P. Soman, "Implementation of a low cost synthetic aperture radar using software defined radio," in *Second International Conference on Computing Communication, and Networking Technologies*, Karur, India, Jul. 29–31, 2010, pp. 1–7.
- [5] *Radar Handbook*, M. I. Skolnik Ed., 3rd ed. New York, NY: McCraw-Hill, 2008.